Polym. Korea, Vol. 47, No. 3, pp. 361-368 (2023)
https://doi.org/10.7317/pk.2023.47.3.361

ISSN 0379-153X(Print)
ISSN 2234-8077(Online)

내마모성 부품의 DLP 3D 프린팅을 위한 흄 실리카를 이용한 레진의 보강

황보현우 · 김현우*, · 권순훈*,**,† · 전석진†**

금오공과대학교 고분자공학과, *금오공과대학교 컨설팅학과
**TMC 융합컨설팅법인

(2023년 1월 18일 접수, 2023년 2월 1일 수정, 2023년 2월 13일 채택)

Reinforcing Resins with Fumed Silica for DLP 3D Printing of Abrasion-resistant Parts

Hyeonwoo Hwangbo, Hyun Woo Kim*,, Soon Hoon Kwon*,**,†, and Seog-Jin Jeon*,†**

Department of Polymer Science and Engineering, Kumoh National Institute of Technology, Gumi, Gyeongbuk 39177, Korea
**Department of Consulting, Kumoh National Institute of Technology, Gumi, Gyeongbuk 39177, Korea*
***TMC convergence consulting corporation, Daegu 42012, Korea*

(Received January 18, 2023; Revised February 1, 2023; Accepted February 13, 2023)

초록: Digital light processing(DLP) 3D 프린팅은 100 μm 미만의 높은 프린팅 해상도로 정교한 산업용 부품 제작이 가능하여 많은 관심을 받아왔다. 다양한 산업적 응용 중 내마모성 부품의 제작은 제작단가 절감과 환경 친화성으로 인해 3D 프린팅이 적용되었을 때 가장 효용성이 높은 분야 중 하나이다. 내마모성 부품의 제작에 적용되어 온 기존의 공정인 절삭가공에서는 버려지는 재료의 분율이 너무 높으며, 내마모성에 의한 가공 과정에서 절삭공구의 빠른 마모에 의해 가공 비용이 증가하게 된다. 내마모성 부품을 3차원 가공으로 성형하면 버려지는 부분과 절삭공구 비용이 획기적으로 감소하여 제작단가 절감 효과가 매우 높아질 수 있다. 본 연구에서는 3D 프린팅 레진 조성물에 흄 실리카를 넣어 내마모성을 보강하였고, 출력물의 기계적 물성 및 내마모성을 평가하였다. 흄 실리카가 3 wt% 첨가된 최적화된 조성물은 10000 싸이클의 Taber 시험에서 실리카를 포함하지 않은 조성물에 비해 중량 감소가 1/3로 감소하였고, 동시에 충격강도는 3배 증가하였다. 최종적으로, 최적화된 조성물을 이용하여 1-2 mm의 톱니를 갖는 기어를 프린팅함으로써 정교한 출력이 가능함을 검증하였다. 제안된 3D 프린팅을 이용한 내마모성 부품 제작기술은 버려지는 재료와 가공비용을 절감하여 가공 과정에서의 탄소 발자국을 줄이는데 기여할 것으로 기대한다.

Abstract: Digital light processing (DLP) 3D printing is attracting much attention for its ability to fabricate sophisticated industrial parts due to its excellent layer resolution of less than 100 μm. Among various industrial applications, the area where 3D printing benefits the most is the production of abrasion-resistant parts due to cost reduction and environmental friendliness. The conventional process employed mainly for the production of abrasion-resistant parts is based on cutting and grinding, which leaves a significant amount of discarded residues. In addition, the rapid wear of cutting and grinding tools highly increases machining costs. 3D printing of abrasion-resistant parts can minimize discarded parts and drastically reduce the machining costs by eliminating cutting and grinding costs. In this study, we reinforced 3D printing resins with fumed silica and confirmed the enhancement in abrasion resistance. For an abrasion test of 10000 cycles, the optimal composition of fumed silica, 3 wt%, reduced the weight loss during the Taber test to 1/3, and the impact strength increased about three times compared to the case in which silica was not introduced. We finally confirmed that the sophisticated parts could be fabricated using DLP 3D printing of fumed silica containing resins by printing gears with teeth of 1-2 mm. 3D printing technology suggested for the manufacture of abrasion-resistant parts is expected to contribute to lowering the carbon footprint in the manufacturing process through the reduction of discarded wastes and machining costs.

Keywords: abrasion-resistant, fumed silica, reinforced resin, light processing, 3D printing.

†To whom correspondence should be addressed.
sjjeon@kumoh.ac.kr, ORCID 0000-0002-3372-6532
hanulksh@naver.com, ORCID 0000-0003-4226-4824

Introduction

High abrasion-resistant materials contribute to prolonging the life of components in all industrial applications.[1,2] In particular, industrial parts such as bearings, gears, bushings, seals, and skirts undergo wear due to repeated contact and friction. To alleviate this problem, high abrasion-resistant and low coefficient of friction polymers such as polyoxymethylene, polyamide, HDPE, or nanocomposites thereof have been used.[3,4] On the one hand, the abrasion resistance of these polymers contributes to prolonging the life of the parts, but on the other hand, the high abrasion resistance causes the cutting and grinding tools to wear out at a high rate during the cutting and grinding process of these polymers. Therefore, in the processing of abrasion-resistant parts, it is required to introduce an expensive cutting and grinding tool that is strong and has high abrasion resistance, and frequent replacement of the tools increases machining costs. In addition, many parts are discarded by cutting and grinding, which acts as another factor increasing the manufacturing costs. Therefore, it is very desirable to apply a bottom-up approach, such as 3D printing, rather than a top-down approach based on cutting in order to reduce manufacturing costs in the fabrication of abrasion-resistant parts.[5-7]

Recently, 3D printing has developed into various methods, such as fused deposition modeling (FDM) and digital light processing (DLP). In particular, DLP 3D printing, which is based on layer-by-layer photocuring of a liquid resin, is superior to other 3D printing techniques, such as FDM, in manufacturing sophisticated parts due to its high printing resolution of less than 100 μm.[8-10] In addition, DLP 3D printing based on the deposition of faces is superior in terms of the production yield to FDM 3D printing based on the deposition of lines, and the physical properties of DLP products can be widely modified with the help of the photochemistry of various resin compositions. For example, different resin compositions enable a wide range of modulus control of the 5 order, from soft hydrogels with a modulus of several hundred kPa to rigid dental models with a modulus of several GPa.[11-17]

A commonly used resin composition is an acrylate-based composition composed of a combination of oligomers, monomers, photoinitiators, etc. Representative oligomers are epoxy and polyurethane having an acrylate functional group, which highly affects in the physical properties and reduces shrinkage due to cross-linking. As a monomer, acrylate with the functionality between 1 and 5 is introduced, and serves to control the crosslinking density and viscosity. There has been no reports on DLP 3D printing of a resin composition targeting abrasion resistance. For a photocurable resin composition for film coating, Marasinghe et al. suggested that when the function is 3 or more, the increase in functionality contributes to the improvement of abrasion resistance.[18] In addition, it has been reported that the abrasion resistance is improved by introducing inorganic particles such as silica into the photocurable composition for film coating.[19-21] In general, it is known that inorganic particles in polymer composite materials contribute to the improvement of abrasion resistance by resisting micro-crack initiation and propagation. For example, Malaki *et al*. have been reported that the abrasion resistance is improved by 3 times with 6% of fumed nanosilica.[19] However, research on DLP 3D printing resin compositions for improving abrasion resistance is largely unexplored.

In this study, it was confirmed that abrasion resistance was increased by formulation and printing a resin composition for DLP 3D printing in which multifunctional monomers and fumed silica were introduced. Fumed silica was completely mixed with the resin composition to form a transparent phase, which suppressed scattering and did not impair printing quality during UV cross-linking. Through the Taber abrasion test of the 3D printed specimen, it was confirmed that the weight loss was reduced by 1/3 compared to the composition without silica, and the impact strength was increased by 3 times. Research on 3D printing of abrasion-resistant parts is essential for establishing a sustainable production environment and is expected to contribute to carbon neutrality.

Experimental

Materials. Difunctional urethane acrylate oligomer (UA, M_W = 2000 g/mol) was purchased from Sartomer (US). Trimethylolpropane triacrylate (TMPTA) and isobornyl acrylate (IBA) were purchased from TCI chemicals (Japan). Fumed silica (FS) with an average particle size of 0.2-0.3 μm was purchased from Sigma Aldrich (US). Phenylbis(2,4,6-trimethyl benzoyl) phosphine oxide (BAPO) and 2,5-bis(5-tert-butyl-2-benzoxazoyl)thiophene (TBT) were purchased from TCI chemicals (Japan) for the use as a photoinitiator and optical blocker.

Resin Formulation for DLP 3D Printing. Resins for printing were prepared by macroscopic mixing of acrylates, FS, BAPO, and TBT with a wood stick and microscopic mixing with an ultrasonicator, and stored overnight in a dark room to remove air bubbles. The ultrasonication was performed at least 3 hours for sufficient dispersion of FS in the resin. Four resin

Table 1. Summary of Name and Composition of Formulated Resins (unit: wt%)

Resin name	UA	TMPTA	IBA	FS	BAPO	TBT
UI	30	-	70	-	0.45	0.164
UTI	29.386	50	20	-	0.45	0.164
UTIS1	28.386	50	20	1	0.45	0.164
UTIS2	27.386	50	20	2	0.45	0.164
UTIS3	26.386	50	20	3	0.45	0.164
UTIS4	25.386	50	20	4	0.45	0.164

compositions were prepared, and the contents of each composition are summarized in Table 1. For convenience, the name of the resin composition was named after the first letter of the acrylates contained. For example, the composition containing UA and IBA was referred to as UI.

DLP 3D Printing. A DLP 3D printer (CGR, Wanhao, China) was used, and the slicing operation for printing was performed using software (Chitubox, Wanhao, China). The wavelength of UV was 405 nm and the exposure time for each layer was set to 10 seconds. Typically, 3D printing was performed after filling the vat with 100 mL of resin. Printed products were washed with ethanol and post-cured with UV for 1 hour to fully cross-link unreacted acrylates.

Characterization. Specimens for the tensile test were prepared in the form of a dog bone according to ASTM D638IV. Specimens were printed with a thickness of 3.4 mm and the tensile test was performed using a Universal Testing Machine (UTM, AG-Xplus, Shimadzu, Japan) with a strain rate of 5 mm/min and an applied load of 50 kN. At least ten samples were measured to obtain the average modulus, ultimate strength, and elongation at break. Specimens for the Taber abrasion test were prepared in the form of a disc according to ASTM D4060. The thickness and diameter of the disc were 5 mm and 100 mm, respectively. Due to the limitation of the printing size of the 3D printer used, two printed semi-discs were attached to form a disc and leveled carefully using a sandpaper (Figure S1). The rotation speed of the wheel was 100 rpm with 100 g of an applied load for both sides. The weight loss was measured every 2000 rotations, and finally up to 10000 rotations. The transmittance was measured using a UV-vis spectrometer (Flame, Ocean insight, US). The viscosity of resins was measured using a cone-plate rheometer (Discovery HR30, TA instrument, US) in the shear rate range of 0.003 to 600 s^{-1} at 20 ℃. The surface of the specimens after the abrasion test was observed using a scanning electron microscope (SEM, JSM-6500F, JEOL, Japan) operated at an accelerating voltage of 15 kV. The specimen was coated with a thin layer of Pt prior to the SEM observation. From the measured SEM photograph, the area ratio of the smooth surface after the abrasion test was analyzed using image J. The impact resistance of the printed samples was evaluated by the Izod impact test (92T, Tinius Olsen, US) to ASTM D256 test procedure. The dimension of the samples was 63.5 × 12.7 × 3.2 mm with a 2.5 mm V-shaped notch depth. Each impact strength is the average value of 10 samples.

Results and Discussion

Mechanical Properties and Abrasion Resistance of 3D Printed Products Using the Base Resin. In order to prepare a resin composition for DLP 3D printing with high abrasion resistance, an appropriate resin composition for printing was studied. DLP 3D printing is a method of forming a three-dimensional structure using layer-by-layer curing of UV-curable resin. After one layer of UV exposure, the fresh resin should smoothly move to the UV curing sites to help form a new layer. To this end, the viscosity of the resin must be suitable for printing. It has been reported that DLP 3D printing can be properly performed at the viscosity of less than 5 Pa·s at room temperature.[22] IBA used as a monomer acts as an effective diluent with 10 mPa·s at room temperature. The viscosity of all resins used in the experiment was between 0.137 and 0.837 Pa·s and was suitable for 3D printing.

Polyurethane is known to have excellent mechanical properties, internal hydrolysis, and thermal stability by the microscopic phase separation of soft oligodiol and hard isocyanate.[23,24] In this study, the UA was used as an oligomer with the expectation of those excellent mechanical properties, and IBA with rigid bulky cycloalkyl group was used as a monomer to improve toughness and rigidity. We 3D-printed dogbone-shape specimens of UI and UTI and evaluated mechanical properties from the tensile test. A typical stress-strain curve is shown in Figure 1(a), and the average modulus, ultimate tensile stretches,

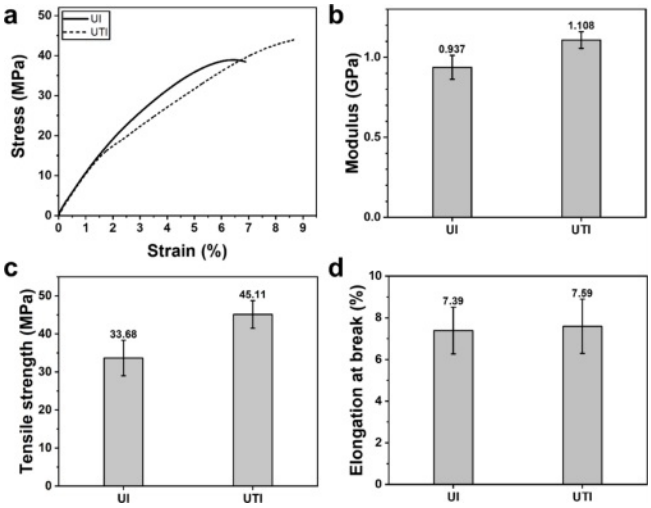

Figure 1. (a) Typical stress-strain curves; (b) modulus; (c) tensile strength; (d) elongation at break of 3D printed UI and UTI. Numbers above bars are averaged values.

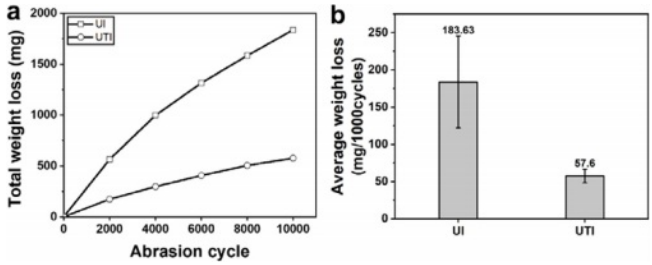

Figure 2. (a) Total weight loss; (b) average weight loss of 3D printed UI and UTI by Taber abrasion test. Numbers above bars are averaged values.

and elongation at break were obtained from tensile test results of 10 specimens. The modulus, ultimate tensile strength, and elongation at break of UI were 0.937 GPA, 33.68 MPA, and 7.39%, respectively (Figure 1(b)-(d)). For the formulation of UTI, we increased the crosslink density by lowering the content of IBA having a functionality of 2 from 70 to 20 wt%, and replacing the reduced content with TMPTA with a functionality of 3 with the expectation of achieving improved mechanical properties. The modulus, ultimate tensile strength, and elongation at break of UTI were 1.108 GPA, 45.11 MPA, and 7.59%, respectively (Figure 1(b)-(d)). Compared to the UI specimen, modulus and elongation at break were almost no different, while ultimate tensile strength increased by about 34%.

The Taber abrasion test was performed to compare the abrasion resistance of UI and UTI samples. For a total of 10000 rotations, the weight loss was measured every 2000 rotations, and the results are shown in Figure 2(a). The weight loss after 10000 rotations was 1836.3 mg for UI and 576.4 mg for UTI. As a result of comparing the average weight loss per 1000 rotations from the weight loss measured every 2000 rotations, UI showed 183.63 mg/1000 rotation and UTI showed 57.6 mg/1000 rotation (Figure 2(b)), which means that the abrasion resistance was improved by 3.19 times. There was no significant difference between the two resins in modulus, elongation, and tensile strength, but UTI showed a significant improvement in abrasion resistance. Since UI and UTI are very similar in all mechanical properties, it can be inferred that the improvement of abrasion resistance is dominated by the increase of crosslink density. Theoretically, the crosslinking density is proportional to the concentration and functionality of the crosslinking agent,[25] and since IBA having a functionality of 1 is replaced with TMPTA having a functionality of 3, a 3-fold increase in the crosslinking density is expected with respect to the content of the crosslinking agent in which IBA is replaced with TMPTA. Muratoglu *et al*. have reported that the wear rate increases as the molecular weight between crosslinks increases or the crosslink density decreases, which is consistent with our results.[26]

Optical and Rheological Properties of Fumed Silica Containing Resins. We used fumed silica as a filler to reinforce resins because of (i) the rich hydrogen bonding donor (-OH) on their surface, (ii) its large surface area (~200 m^2/g), (iii) optical transparency, and (iv) cost-effectiveness. The rich hydrogen bonding donor and large surface area are advantageous for strengthening adhesion with polyurethane, and the optical transparency is important for the high resolution photo-curing. In addition, the relatively low cost of fumed silica reduces the cost of 3D printing. We formulated a series of FS-containing resins, UTIS1, UTI2, UTIS3, and UTIS4, based on the composition of UTI resin with high abrasion resistance. The number at the end of FS containing resins' name indicates the FS content in weight percent, and the average particle size of FS was 0.2-0.3 μm. For the addition of silica, the resin initially appeared cloudy (Figure 3(a)), but it recovered its original transparent state after 1 hour of ultrasonication (Figure 3(b)). The transmittance of resins is almost uniform for the wavelength region of 450-650 nm, as shown in Figure 3(c). In the wavelength region, the average transmittances of UTI, UTIS1, UTIS2, UTIS3, and UTIS4 were 89.1, 87.6, 85.3, 84.0, and 83.9%, respectively. The decrease in average transmittance by increasing the FS content was not significant and did not affect the 3D printing conditions. The rheological property of the FS-containing resins was dependent on the FS content and shear

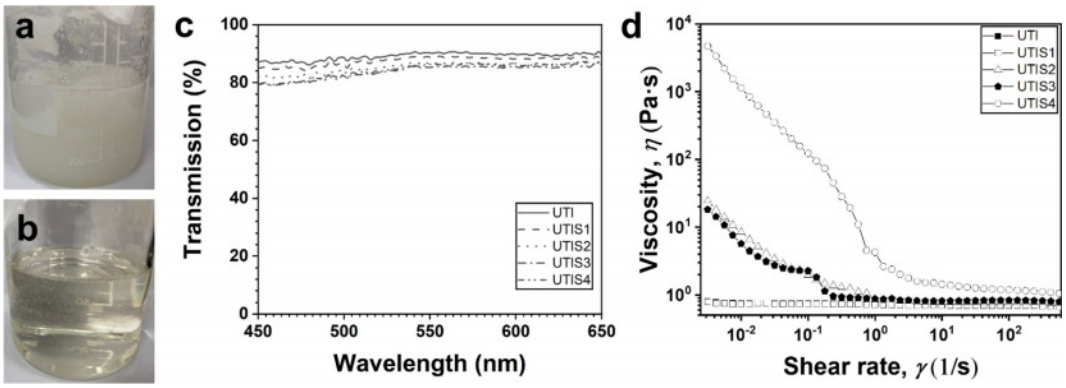

Figure 3. (a) Image of resin immediately after the addition FS; (b) after 1 hour of ultrasonication; (c) transmission spectra; (d) viscosity according to shear rate of UTI, UTIS1, UTIS2, UTIS3, and UTIS4 resins.

rate. UTI and UTIS1 resins showed almost uniform viscosity for the whole shear rate regions measured (Figure 3(d)). On the other hand, for the FS-containing resins with the FS content of between 2 and 4 wt%, shear thinning behavior was observed for the shear rate lower than 1 s^{-1}, and the viscosity for the shear higher than 1 s^{-1} was almost uniform. Though the viscosity of UTIS2 and UTIS3 was higher than the viscosity limit of printable resins, 5 Pa·s, for the shear rate lower than 10^{-2} s^{-1}, we could confirm that they were printable by actual printing test. However, UTIS4 showed shear thinning behavior at the whole shear rate region measured, and the viscosity was higher than the viscosity limit at the shear rate lower than 1 s^{-1}. Without shear, UTIS4 behaved like highly viscous gel and was not printable. Therefore, we pursued printing the FS-containing resins with the FS content lower than 4 wt%.

Abrasion Resistance and mEchanical Properties of 3D Printed Products Using Fumed Silica Containing Resins. We performed the Taber abrasion test on printed specimens from UTIS1 and UTIS3 and compared the results with specimens printed from UTI. The disc specimen before and after the abrasion test is shown in Figure 4(a), and half of the disc after the abrasion test was separated for SEM observation. The weight loss after 10000 rotations of UTI, UTIS1, and UTIS3 were 576.4, 381.1, and 238.2 mg, and the weight loss was slightly reduced as the abrasion cycle increased (Figure 4(b)). As a result of calculating the average weight loss per 1,000 rotations, UTI, UTIS1, and UTIS3 showed 57.6, 38.1, and 23.8 mg/1,000 rotation, respectively (Figure 4(c)). UTIS3 showed about 60% reduced weight loss compared to UTI. The surface of the abraded specimens was observed using SEM for the analysis of abrasion behavior. For UTI specimens, the surface was very rough, and only a few surfaces remained smooth. For UTIS1

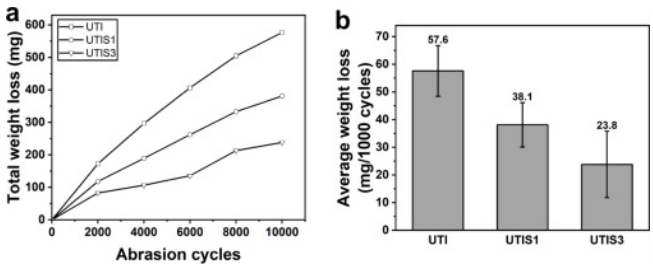

Figure 4. (a) Total weight loss; (b) average weight loss of 3D printed UTI, UTIS1, and UTIS3 by Taber abrasion test. Numbers above bars are averaged values.

and UTIS3 specimens, more smooth surfaces without abrasion were found than in UTI specimens (Figure 5). As a result of calculating the ratio of the area remaining smooth after the 10,000 cycles of the Taber abrasion test from 20 SEM images of the surface of UTI, UTIS1, and UTIS3 (*e.g.*, Figure S2), it was 17.7, 29.5, and 59.5%, respectively. This result indicates that UTIS1 and UTIS3 have 1.7 and 3.4 times higher smooth area ratio than UTI, respectively. This means that the abrasion resistance of UTIS1 and UTIS3 was improved by the addition of FS, which is consistent with the Taber abrasion test results. The enhancement in abrasion resistance can be explained by the enhanced adhesion and physical properties of fumed silica. Fumed silica provides large interfacial contact with polyurethane due to its large surface area (200 m^2/g), and hydrogen bonding formed between the carbonyl group of polyurethane and the hydroxyl group of fumed silica strengthens the adhesion between them,[27] which suppresses nucleation of cracks at their interfaces. In addition, rigid particles such as silica impede the propagation of fatigue cracks that occur during abrasion according to the crack pinning mechanism,[28,29] and silica acts as a solid lubricant to reduce abrasion due to its low friction

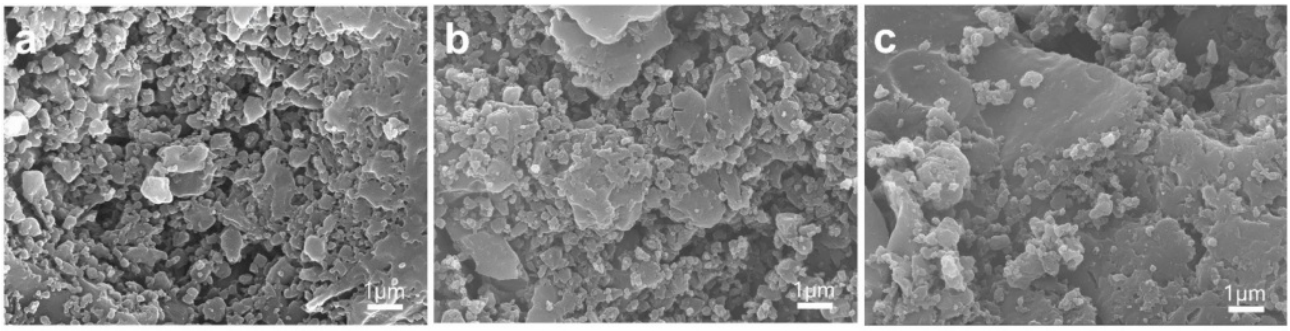

Figure 5. Surface SEM images of 3D printed (a) UTI; (b) UTIS1; (c) UTIS3 after 10000 cycles of Taber abrasion test.

coefficient, 0.1-0.3.

Improvement of mechanical property by the addition of FS was studied by the tensile test of UTI and UTI3. The modulus, ultimate tensile strength, and elongation at break of UTIS3 specimens were 1.334 GPa, 43.69 MPa, and 6.47%, respectively (Figure 6(a)-(c)). Compared to UTI specimens, the modulus increased by 20%, but decreased by 3.3% and 17%. On the other hand, As a result of measuring the impact strength through the Izod test, UTI and UTIS3 were 11.3 J/m and 32.3 J/m, respectively, indicating that UTIS3 had 2.8 times higher impact strength (Figure 6(d)). While the modulus, ultimate tensile strength, and elongation at break did not show a significant difference between UTI and UTIS3, UTIS3 showed a remarkable improvement in the impact strength, which may be enabled by sufficient interfacial adhesion between the polymer matrix and silica filler. It has been reported that the impact strength of polyurethane-fumed silica composites decreases with increasing silica content due to a localized stress build-up on the periphery of silica.[30] However, the enhanced wetting induced by selective interaction between matrix and fillers is known to improve mechanical properties, including impact strength.[31] It is noteworthy that the impact strength was increased without any chemical modification to improve wetting in our case. We speculate that the layer-by-layer curing of fine slices smaller than 100 μm by DLP 3D printing provides uniform dispersion of silica everywhere in the product and thus contributes to the enhanced wetting and improvement in the impact strength.

3D Printing of Finely Shaped Parts Using Fumed Silica Containing Resin. Finally, we used UTIS3 resin to 3D print gears, which are representative industrial parts that require both abrasion resistance and sophisticated shapes (Figure 7). The smallest part is the inner tooth of the gear in Figure 7(a) with a width of about 1.7 mm, and the thickness of the gears shown in Figures 7(a)-(c) are 8 mm, 4 mm, and 4 mm, respec-

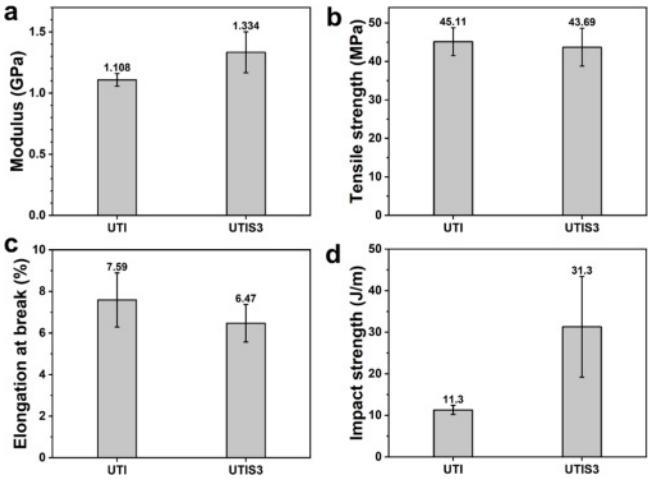

Figure 6. (a) Modulus; (b) tensile strength; (c) elongation at break; (d) impact strength of 3D printed UTI and UTIS3. Numbers above bars are averaged values.

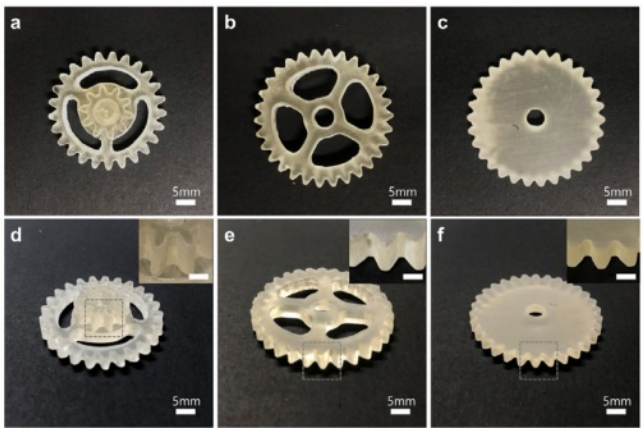

Figure 7. (a-c) Top-view images of different shaped gears that were 3D printed using UTIS3; (d-f) Side-view images of (a-c) at an angle of inclination. Insets are enlarged images of gray dashed areas in (a-c). Scale bars are 2.5 mm.

tively. The advantage of DLP 3D printing is that it can print multiple prints at once in proportion to the area of the UV exposure area because it is based on layer-by-layer deposition. The exposure area of the 3D printer used in this experiment was 192 mm × 120 mm, and in the case of Figure 7(a) gear, 15 pieces could be printed at once. All of the gears were printed very precisely, and even if the image was enlarged (Figures 7(d)-(f) insets), a very smooth side without any noticeable texture was obtained. The printability of the other FS-containing resins, UTIS1 and UTIS2, was also tested by printing gear, and we could confirm that high resolution printing was possible for all FS-containing resins (Figure S3). Through this demonstration, we could confirm the possibility of DLP 3D printing to manufacture industrial parts that need both sophistication and abrasion resistance.

Conclusions

We successfully performed DLP 3D printing using FS-containing resins and assessed the abrasion resistance of printed products. We prepared a resin composition containing FS of 4 wt% or less and investigated transmittance and viscosity to evaluate whether the resin containing FS is suitable for DLP 3D printing. All the resins containing 4 wt% or less of FS were almost transparent, with an average visible light transmittance of 84% or more. The resin without FS and 1 wt% of FS showed Newtonian behavior, but the resin with FS of 2 wt% or more showed shear thinning. In particular, 4 wt% of FS resin exhibited too high viscosity at a shear rate lower than 1 s^{-1}, which made printing impossible. Therefore we pursued 3D printing using resins containing FS of 3 wt% or less. For the Taber abrasion test, UTIS3, the resin containing 3wt% FS, showed the best abrasion resistance. The average weight loss of UTIS3 products was reduced by 1/3 compared to products from UTI, the resin without FS. Also, from the surface SEM, the area ratio remained smooth for UTIS3 increased 3.4 times compared to the UTI. In addition, UTIS3 products exhibited an impact strength 2.8 times higher than that of UTI products, indicating that interfacial adhesion between silica and polymer matrix was well formed. Finally, we successfully pursued 3D printing of gears, which are industrial parts that require sophistication and abrasion resistance at the same time. Here, we proposed a method for manufacturing sophisticated and abrasion-resistant parts with reduced discarded wastes and machining costs, and thus expect that the 3D printing technology will contribute to reducing carbon footprints in the manufacturing process.

Acknowledgments: This research was supported by National University Development Project (2020).

Conflict of Interest: The authors declare that there is no conflict of interest.

Supporting Information: Information is available regarding the specimen before and after Taber abrasion test and the calculation of the area ratio of the smooth surface are after Taber abrasion test. The materials are available *via* the Internet at *via* the Internet at http://journal.polymer-korea.or.kr

References

1. Zhai, W.; Bai, L.; Zhou, R.; Fan, X.; Kang, G.; Liu, Y.; K. Zhou. Recent Progress on Wear-Resistant Materials: Designs, Properties, and Applications. *Adv. Sci.* **2021**, 8, 2003739.
2. Meng, J.; Zhang, P.; Wang, S. Recent Progress of Abrasion-resistant Materials: Learning from Nature. *Chem. Soc. Rev.* **2016**, 45, 237-251.
3. Myshkin, N. K.; Kovalev, A. V. Friction and Wear of Polymers and Polymer Composites; ASM International: Materials Park, 2017.
4. Abdelbary, A. Wear of Polymers and Composites; Woodhead Publishing: Sawston, 2015.
5. Ligon, S. C.; Liska, R.; Stampfl, J.; Gurr, M.; Mülhaupt, R. Polymers for 3D Printing and Customized Additive Manufacturing. *Chem. Rev.* **2017**, 117, 10212-10290.
6. Ngo, T. D.; Kashani, A.; Imbalzano, G.; Nguyen, K. T. Q.; Hui, D. Additive Manufacturing (3D Printing): A Review of Materials, Methods, Applications, and Challenges. *Compos. B. Eng.* **2018**, 143, 172-196.
7. Pal, A. K.; Mohanty, A. K.; Misra, M. Additive Manufacturing Technology of Polymeric Materials for Customized Products: Recent Developments and Future Prospective. *RSC Adv.* **2021**, 11, 36398-36438.
8. Maines, E. M.; Porwal, M. K.; Ellison, C. J.; Reineke, T. M. Sustainable Advances in SLA/DLP 3D Printing Materials and Processes. *Green Chem.* **2021**, 23, 6863-6897.
9. Akyalcin, S.; Rutkowski, P.; Arrigo, M.; Trotman, C. A.; Kasper, F. K. Evaluation of Current Additive Manufacturing Systems for Orthodontic 3-dimendional Printing. *Am. J. Orthod. Dentofacial Orthop.* **2021**, 160, 594-602.
10. Hwangbo, H.; Jeon, S.-J. Digital Light Processing 3D Printing of Multi-Materials with Improved Adhesion using Resins Containing Low Functional Acrylates. *Korean J. Chem. Eng.* **2022**, 39, 451-459.
11. Ge, Q.; Jian, B.; Li, H. Shaping Soft Materials via Digital Light Processing-based 3D Printing: A Review. *Forces Mech.* **2022**, 6, 100074.
12. Zhang, X. N.; Zheng, Q.; Wu, Z. L. Recent Advances in 3D

Printing of Tough Hydrogels: A Review. *Compos. B. Eng.* **2022**, 238, 109895.
13. Herzberger, J.; Sirrine, J. M.; Williams, C. B.; Long, T. E. Polymer Design for 3D Printing Elastomers: Recent Advances in Structure, Properties, and Printing. *Prog. Polym. Sci.* **2019**, 97, 101144.
14. Thrasher, C. J.; Schwartz, J. J.; Boydston, A. J. Modular Elastomer Photoresins for Digital Light Processing Additive Manufacturing. *ACS Appl. Mater. Interfaces* **2017**, 9, 39708-39716.
15. Lin, C.-H.; Lin, Y.-M.; Lai, Y.-L.; Lee, S.-Y. Mechanical Properties, Accuracy, and Cytotoxicity of UV-polymerized 3D Printing Resins Composed of Bis-EMA, UDMA, and TEGDMA. *J. Prosthet. Dent.*, **2020**, 123, 349-354.
16. Shah, D. M.; Morris, J.; Plaisted, T. A.; Amirkhizi, A. V.; Hansen, C. J. Highly Filled Resins for DLP-based Printing of Low Density, High Modulus Materials. *Addit. Manuf.* **2021**, 37, 101736.
17. Kebler, A.; Hickel, R.; Ilie, N. *In vitro* Investigation of the Influence of Printing Direction on the Flexural Strength, Flexural Modulus, and Fractographic Analysis of 3D-printed Temporary Materials. *Dent. Mater. J.* **2021**, 40, 641-649.
18. Marashinghe, L.; Croutxé-Barghorn, C.; Allonas, X.; Criqui, A. Effect of Reactive Monomers on Polymer Structure and Abrasion Resistance of UV Cured Thin Films. *Prog. Org. Coat*. **2018**, 118, 22-29.
19. Malaki, M.; Hashemzadeh, Y.; Tehrani, A. F. Abrasion Resistance of Acrylic Polyurethane Coatings Reinforced by Nano-Silica. *Prog. Org. Coat.* **2018**, 125, 507-515.
20. Palraj, S.; Selvaraj, M.; Maruthan, K.; Rajagopal, G. Corrosion and Wear Resistance Behavior of Nano-Silica Epoxy Composite Coatings. *Prog. Org. Coat.* **2015**, 81, 132-139.
21. Bahadur, S.; Gong, D.; Anderegg, J. W. Tribochemical Studies by XPS Analysis of Transfer Films of Nylon 11 and Its Composites Containing Copper Compounds. *Wear* **1993**, 165, 205-212.
22. Taormina, G.; Sciancalepore, C.; Messori, M.; Bondioli, F. 3D Printing Processes for Photocurable Polymeric Materials: Technologies, Materials, and Future Trends. *J. Appl. Biometer. Funct. Mater.* **2018**, 16, 151-160.
23. Howard, G. T. Biodegradation of Polyurethane: A Reivew. *Int. Biodeterior. Biodegrad.* **2022**, 49, 245-252.
24. Christenson, E. M.; Anderson, J. M.; Hiltner, A. Biodegradation Mechanisms of Polyurethane Elastomers. *Corrosion Eng. Sci. Technol.* **2007**, 42, 312-323.
25. Xue, W.; Huglin, M. B.; Jones, T. G. J. Swelling and Network Parameters of Crosslinked Thermoreversible Hydrogels of Poly(*N*-ethylacrylamide). *Eur. Polym. J.* **2005**, 41, 239-248.
26. Muratoglu, O. K.; Bragdon, C. R.; O'Connor, D. O.; Jasty, M.; Harris, W. H.; Gul, R.; McGarry, F. Unified Wear Model for Highly Crosslinked Ultra-High Molecular Weight Polyethylenes (UHMWPE). *Biomaterials* **1999**, 20, 1463-1470.
27. Nuñes, R.; Fonseca, J.; Pereira, M. Polymer-filler Interactions and Mechanical Properties of a Polyurethane Elastomer. *Polym. Test.* **2000**, 19, 93-103.
28. Green, D. G.; Nicholson, P. S.; Embury, J. D. Fracture of a Brittle Particulate Composite, Part 2: Theoretical Aspects. *J. Mater. Sci.* **1979**, 14, 1657-1661.
29. Imanaka, M.; Takeuchi, Y.; Nakamura, Y.; Nishimura, A.; Iida, T. Fracture Toughness of Spherical Silica-filled Epoxy Adhesives. *Int. J. Adhes. Adhes.* **2001**, 21, 389-396.
30. Yang, Z.-G.; Zhao, B.; Qin, S.-L.; Hu, Z.-F.; Jin, Z.-K.; Wang, J.-H. Study on the Mechanical Properties of Hybrid Reinforced Rigid Polyurethane Composite Foam. *J. Appl. Polym. Sci.* **2004**, 92, 1493-1500.
31. Rong, M. Z.; Zhang, M. Q.; Ruan, W. H. Surface Modification of Nanoscale Fillers for Improving Properties of Polymer Nanocomposites: A Review. *Mater. Sci. Technol.* **2006**, 22, 787-796.